



Published in final edited form as:

Int J Cancer. 2012 September 15; 131(6): 1351–1359. doi:10.1002/ijc.27380.

Preclinical Evaluation of Mab CC188 for Ovarian Cancer Imaging

M Xu¹, MP Rettig², G Sudlow¹, B Wang³, WJ Akers¹, D Cao³, DG Mutch⁴, JF DiPersio², and S Achilefu^{1,5}

¹Department of Radiology, Washington University School of Medicine, St. Louis, MO 63110, USA

²Siteman Cancer Center, Division of Oncology, Washington University School of Medicine, St. Louis, MO 63110, USA

³Department of Pathology and Immunology, Washington University School of Medicine, St. Louis, MO 63110, USA

⁴Department of Obstetrics and Gynecology, Division of Gynecologic Oncology, Washington University School of Medicine, St. Louis, MO 63110, USA

⁵Department of Biochemistry & Molecular Biophysics, Washington University School of Medicine, St. Louis, MO 63110, USA

Abstract

Cancer stem cells (CSCs) have been successfully isolated from solid tumors and are believed to be initiating cells of primary, metastatic and recurrent tumors. Imaging and therapeutic reagents targeted to CSCs have potential to detect subclinical tumors and completely eradicate the disease. Previously, we have demonstrated that Mab CC188 binds to colon cancer CD133- and CD133+ (CSCs) cells. In this study, we examined the reactivity of Mab CC188 to ovarian cancer cells including CD133+ cells and primary tumor tissues using immunofluorescence staining methods and tissue microarray technique. We also explored the feasibility of using NIR dye-labeled Mab CC188 probe to image ovarian tumors in vivo. Mab CC188 stains both CD133- and CD133+ cells of ovarian cancer. Tissue microarray analysis reveals that 75% (92/123) of ovarian cancer cases are positively stained with Mab CC188. Weak positive (\pm), positive (+), strong positive (++) and very strong positive (+++) stains are 14.8%, 3.7%, 11% and 24.4% respectively. In contrast, Mab CC188 staining is low in normal cells and tissues. In vivo study show that significant amounts of the probe accumulates in the excretion organs in the early period post injection. At 24 hours, the imaging probes have largely accumulates in the tumor, while the intensity of the imaging probe decreases in the liver. The tumor uptake was still evident at 120 hours post injection. Our work suggests that Mab CC188 based imaging and therapeutic reagents are capable of detecting early stage ovarian tumors and effectively treating the tumor.

Keywords

Monoclonal antibody; Cancer stem cell; Ovarian cancer; Optical imaging

Introduction

Despite advances in the diagnosis and treatment of cancer, the death rate for ovarian cancer has not changed much in the last 50 years [1]. Ultimately 21,000 women will be diagnosed

Corresponding authors: Mai Xu and Samuel Achilefu, Department of Radiology, 4525 Scott Avenue, St. Louis, MO 63110, USA. Fax: +1 314-747-5191; Tel: +1 314-362-8599; xum@mir.wustl.edu or achilefu@mir.wustl.edu.

No potential conflicts of interest were disclosed.

with this disease and 14,000 women will die from it this year in the United States [2]. The high mortality rate is partially due to the late stage at diagnosis. More than 80% of the patients present at either stage III or IV necessitating aggressive treatment regimens such as systemic chemotherapy [3,4]. In these patients the 5-year survival rate is only about 33% [5]. Thus, the high mortality rate at least partially reflects the lack of sensitive and accurate methods for detecting asymptomatic early stage ovarian tumors when survival might be significantly higher [5, 6]. In addition, accurate methods for monitoring the tumor therapeutic response and recurrence post treatment are lacking [7].

In the fight against this devastating disease, tumor circulating markers such as CA-125 and HE4 have been intensively investigated in the clinic to identify and monitor the progression of ovarian cancer. These are particularly useful for monitoring tumor therapeutic response and in detecting recurrence post treatment [8-11]. Although studies have revealed that CA-125 is not tumor specific [12-14], using the strategy of combining multiple serum tumor markers may facilitate the detection of early stage tumors and more accurately predict tumor recurrence [15-18]. Unfortunately, the measurement of serum tumor biological markers cannot be used to assess disease site or volume, which is important in treatment planning [19]. Recent studies have shown that functional imaging with [¹⁸F]-Fluorodeoxyglucose positron emission tomography/computed tomography (FDGPET/CT), may be a more sensitive tool to detect the metabolic activity of tumors, but this method is often unable to identify quiescent (dormant) cancer stem cells (CSCs), which are more aggressive and resistant to therapeutic treatment [2,19].

In recent years, CSCs have been isolated from solid tumors and hypothesized to be the initiating cells of primary, local recurrent and metastatic tumors, and they are responsible for the resistance of tumors to conventional chemo- and radiotherapies [7,20,21]. Therefore, development reagents aimed at CSCs in tumor imaging and targeted therapy holds promise to improve the survival and quality of life for cancer patients, especially for patients with metastatic ovarian cancer for which little progress has been made in recent years [22].

In a previous study, we reported that a carbohydrate antigen recognized by Mab CC188 was expressed on the cell membranes of human colon CSCs and their differentiated progeny, but had limited expression in normal cells and tissues [23]. In the current study, we examined the expression of Mab CC188 binding epitope in ovarian cancer stem (CD133+) cells and their differentiated progeny in vitro, and explored the feasibility of imaging ovarian xenograft tumors using Mab CC188 conjugated with near infrared (NIR) dye in a tumor bearing animal model.

Materials and Methods

Cell lines and cell culture

Human ovarian cancer A2780 cells were cultured in RPMI1640 medium supplemented with 10% FCS (Hyclone), 50 units/ml sodium penicillin, 50 µg/ml streptomycin sulfate (BioWhittaker) and 2 mM glutamine. SKOV-3 human ovarian cancer cells were maintained in DMEM medium supplemented with 10% FCS, 50 units/ml sodium penicillin, 50 µg/ml streptomycin sulfate (BioWhittaker). Mab CC188 hybridoma cells were cultured in Iscove's modified Dulbecco's medium supplemented with 20% fetal bovine serum (Hyclone), 50 units/ml sodium penicillin, 50 µg/ml streptomycin sulfate, 4 mmol/l L-glutamine (BioWhittaker), 1 mmol/l sodium pyruvate (BioWhittaker), and 0.0001% h-mercaptoethanol (Sigma Chemical Co.) for the antibody production. All cells were cultured in a humidified incubator at 37° C with 5% CO₂.

Monoclonal antibody production and purification

Monoclonal antibody (Mab) CC188 was produced by culturing the hybridoma cells in vitro and purified using protein G Sepharose according to the manufacturer's instruction (Amersham Biosciences). Briefly, the supernatant from the hybridoma culture was centrifuged at 14,000 g for 20 minutes at 4°C, filtered through a 0.22- μ m filter to remove fine particles, and the pH was adjusted to 7.0 using equilibration buffer [1 mol/l Tris (pH 9.0)]. The supernatant was passed through a protein G Sepharose column (GE healthcare, Life Sciences) and the column was washed with binding buffer [50 mmol/l Na₂PO₄, 500 mmol/l NaCl (pH 6)] before eluting the antibody with glycine (0.1 mol/l; pH 2.7). The antibody was collected and neutralized in a test tube containing 100 μ l of equilibration buffer (1 mol/l, pH 9.0). Antibody concentration was determined using a UV/vis spectrophotometer (Beckman DU 640).

Immunofluorescent and immunohistochemical staining

To examine the expression of Mab CC188 binding antigen on ovarian cancer cell membranes, we applied immunofluorescent staining assay in cultured cells without fixation and permeation. Under this staining condition, only cell surface molecules can be detected because whole IgG (150 KD) does not passively pass through intact cell membranes. Briefly, we seeded 20,000 cells per well in a Lab-Tek slide and allowed them to continuously culture in an incubator at 37°C for 48 hours. After decanting the culture medium, 50 μ l Mab CC188 at a concentration of 5 μ g/ml was added and incubated for 40 minutes at 37°C. The slide was washed 3x with PBS, and 50 μ l of 1,000x diluted Alexa Flour 488-conjugated goat anti-mouse IgG (Molecular Probe) was added to each well of the Lab-Tek slide. The slide was incubated for another 40 minutes at room temperature. The slide was washed with PBS and observed under a confocal fluorescence microscope (Olympus FV1000).

To test the expression of the Mab CC188 binding epitope in human ovarian cancer tissues, we used ovarian tumor tissue arrays (Biomax). The tissue array slides were deparaffinized in xylene and gradient alcohol. After rehydration, the slides were immersed in antigen retrieval solution [10 mmol/l sodium citrate, 0.05% Tween 20 (pH 6.0)] preheated to 100°C for 20 minutes. The buffer and the slides were cooled to room temperature and the slides were rinsed twice with PBS before incubation in blocking buffer containing 5% goat serum for 30 minutes. The slides were further incubated with a primary antibody at a concentration of 10 μ g/ml for 1 hour at room temperature or overnight at 4°C. After rinsing the slides and blocking with peroxidase blocking solution (3% H₂O₂ in PBS) for 10 minutes, the Avidin-Biotin Complex detection system (Vector Laboratory) was used following the manufacturer's instruction. 3, 3'-Diaminobenzidine (DAB, Vector laboratories) was used as chromogen. The stained slides were dehydrated with gradient alcohol and xylene. Finally, the slides were sealed with mounting medium, coverslipped, and scored independently by two researchers with pathology background using a conventional microscope. Based on the staining intensity, all cases were scored as grade 0 (negative), grade 1 (weak or faint), grade 2 (moderate), grade 3 (strong), and grade 4 (very strong) staining. Based on the cell staining proportion, all cases were classified as no staining, <5%, 6%-25%, 26%-70%, and >71%. A combination of both staining intensity and percentage resulted in the following classifications: (-) negative (grade 0 or no staining); (\pm) weak positive (grade 1 or <5%); and the rest of the cases with grades 2-4 were classified according to the percentage of positively stained cells, (+) moderate positive (6%-25%), (++) strong positive (26%-70%) and (+++) very strong positive (>71%).

To explore the binding of Mab CC188 to ovarian CSCs, we isolated CD133 + cells using a magnetic cell sorting method as described in our previous publication [23]. Briefly, after

trypsinization, 1×10^7 ovarian cancer A2780 and SKOV-3 cells were resuspended in 100 μ l of labeling (separation) buffer [PBS without Ca^{2+} and Mg^{2+} , 0.5% bovine serum albumin, 2 mmol/L EDTA (pH 7.2)]. Biotinylated antibody against CD133/1 (10 μ l) was added to the cell suspension for CD133 + cell magnetic isolation. Subsequently, we added 10 μ l phycoerythrin conjugated antibody 293C3 against CD133/2 (Miltenyi Biotec) and 10 μ l Alexa Fluor 488 conjugated Mab CC188 (5 μ g/ml) to the cell suspension for dual immunofluorescence staining. After refrigerating for 10 minutes and washing, the cell pellets were suspended in 80 μ l of labeling buffer and 20 μ l of anti-biotin MicroBeads, and incubated at 4°C for 15 minutes. The cells (1×10^7) were suspended in 500 μ l separation buffer and loaded onto the column for magnetic separation. After washing the column with 500 μ l separation buffer 3 \times and collecting magnetic bead unlabeled cells, the column was removed from separator (magnetic field) and magnetically labeled (CD133+) cells were collected by flushing the column with 1 ml buffer using the plunger supplied with the CD133 cell isolation kit (Miltenyi Biotec). The both magnetic bead labeled and unlabeled cells were spread on a histological slide and coverslipped for fluorescence microscope observation. To labeled Mab CC188 with Alexa Fluor 488, we followed the manufacturer's instruction (Invitrogen). Briefly, bicarbonate (50 μ l; pH 9.0; 1 mol/L) was added to Mab CC188 (0.5 ml; 2 mg/ml) to optimize the pH for efficient reaction of Alexa Fluor 488 dye and the protein. The antibody solution was transferred to a vial containing the reactive dye and the mixture was incubated for 1 hour at room temperature before passing it through a purification column from the labeling kit. The first fluorescence band was collected for immunofluorescence staining and the second band (free dye) was discarded. For confocal microscopy, cells cultured on Lab-Tek slides were visualized with an Olympus FV1000 microscope after the immunostaining. Dual color, Alexa Fluor 488-conjugated Mab CC188 and phycoerythrin-conjugated Mab 294C3 (Miltenyi), stained slides were analyzed using a sequential program from Olympus FV1000 microscope software.

Labeling of Mab CC188 (IgG) with NIR fluorescent dye for imaging in vivo

For tumor optical imaging in a tumor bearing mouse, we labeled Mab CC188 with NIR dye using an IRDye 800CW Protein Labeling Kit (LI-COR Biosciences, Lincoln, Nebraska) following manufacturer's instructions. Briefly, IRDye dye in a tube was dissolved in 25 μ l of ultra pure water provided in the kit and mixed thoroughly by vortexing. Dye solution (7.2 μ l) from the tube reacted with 1 ml Mab CC188 solution (1 mg/ml, free of ammonium ions, primary amines and preservatives such as sodium azide by dialysis and gel filtration). The mixture was incubated for 2 hours at 20°C with protection from light. The dye-antibody conjugate was isolated from free dye using the Pierce Zeba Desalting Spin Column that came with the labeling kit. To verify the labeling quality, we measured the absorbance of the solution containing conjugates at 280 nm and 780 nm (A280 and A780) and calculated the moles of dye per mole of protein according to the formula provided by LI-COR Biosciences. The labeling ratio of dye/protein is 1-2/1.

Optical imaging of tumor in vivo

BALB/c background nude mice were used in this study (n=2). 1×10^7 A2780 human ovarian cancer cells were injected subcutaneously at left lower abdomen for comparing fluorescence intensity of liver and tumor using optical imaging probe. We purposely allowed the tumor to grow larger (2 cm \times 2.3 cm \times 1.5 cm) to develop ischemic necrosis in the center area of the tumor for measuring the tumor tissue penetration ability of the IgG based imaging probes in vivo. For non-invasive optical imaging, 100 μ g of dye-labeled Mab CC188 in 100 μ l of PBS solution was administered per tumor bearing animal by tail vein injection. The ventral side of the animal was scanned with the Pearl NIR imaging system (LI-COR Biosciences, Lincoln, NE) at indicated time points. At the end of experiment (120 hours post probe injection), ex-vivo biodistribution of the imaging reagents was assessed to

confirm the noninvasive *in vivo* observation. Briefly, mice were euthanized by cervical dislocation under isoflurane anesthesia at 120 hours post injection of the imaging reagent. Aliquots of blood and portions of major organs (heart, kidney, lung, spleen, brain, etc) were harvested, washed with PBS and dabbed dry. The Pearl Imager was used to uniformly excite the tissues and organs at the appropriate wavelengths.

Results

Reactivity of Mab CC188 to human ovarian cancer SKOV-3 and A2780 cells

In a previous study, we demonstrated that Mab CC188 binds to colon cancer cells [23]. To test Mab CC188 binding antigen expression in ovarian cancer cells, we stained Mab CC188 in two human ovarian cancer cell lines, SKOV-3 and A2780. As shown in Figure 1, Mab CC188 stains all the ovarian cancer cells and internalized into the cytoplasm through the cell membrane of cultured (living) cells after incubation with Mab CC188 for 40 minutes at 37°C. As mentioned above, IgG (150 KD) cannot passively pass through intact cell membrane. The internalization requires that Mab CC188 first binds to cell surface receptors or antigens followed by a receptor-mediated endocytosis. The internalization implies that Mab CC188 binding antigen is expressed on the ovarian cancer cell surface. In fixed and permeabilized cells with 4% paraformaldehyde containing 0.2% triton X-100, Mab CC188 binding antigen can be detected in both cell membranes and cytoplasm.

Human ovarian cancer tissue array analysis

To evaluate the antibody for ovarian tumor imaging and targeted therapy, we examined the sensitivity and homogeneity of the antibody to human ovarian cancer using tissue arrays (OVC1501, Biomax, US). The results indicate that 75% (92/123 cases) of ovarian cancer are positively stained with Mab CC188. Weak positive, moderate positive, strong positive and very strong positive are 14.8%, 3.7%, 11% and 24.4% respectively. About 35% of ovarian cancers examined show intense and homogenous staining in all histological types of ovarian cancer (Figure 2).

Expression of the epitope recognized by Mab CC188 on the surface of human ovarian cancer (CD133+) stem cells

Mab CC188 stained all the tumor cells examined (Figure 1). It also reacted with a small fraction of CD133-positive (CSCs) cells. These cells exist as a small fraction of tumor mass and they have been hypothesized to be cancer initiating cells and responsible for cancer recurrence, metastasis and resistance to chemo- and radiotherapies. Based on the hypothesis of CSCs, imaging and therapeutic reagents that target CSCs hold great promise for discovering early stage tumors, potentially localizing subclinical (clinically invisible and palpable) malignant lesions and completely eradicating the disease. As Figure 3 shows, Mab CC188 binds to CD133 + cells from both ovarian cancer cell lines, SKOV-3 and A2780. Notably, all cells stained with Mab 293C3 against CD133 antigen were co-stained with Mab CC188. In contrast, Mab CC188 does not react to peripheral blood mononuclear cells (PBMCs, panel B) and CD34 positive normal hematopoietic cells sorted by flow cytometry (panel C).

Biodistribution and kinetic changes of Mab CC188 labeled with NIR dye imaging probes in vivo

A major motivation for identifying tumor specific binding ligands including antibodies is for the diagnosis and treatment of cancer. Evaluation of imaging and therapeutic reagents in the experimental animal is a critical stage for developing biological reagents for future clinical use. Therefore, we labeled Mab CC188 with a NIR dye IRDye 800CW and monitored the

biodistribution and kinetic changes of the antibody-NIR dye conjugates in ovarian tumor bearing mice. As demonstrated in Figure 4, majority of the imaging probes is eliminated from circulation 24 hr post injection and completely removed from blood pool 48 hr after injection. In addition, the ratios of tumor/gut fluorescence continuously increase post injection. The rapid clearance and tumor specific accumulation of this imaging probe ensures high quality tumor images. Significant amounts of the conjugates accumulate in excretion organs (liver) at 5 minutes, 15 minutes and 1 hour post injection. At 24 hours, the imaging conjugates predominantly accumulated in the tumor, but the intensity of the imaging probes was decreased in the liver (Figure 5A). A significant amount of the imaging probe was still retained in the tumor at 120 hours post injection (Figure 5B). Quantitative analysis clearly shows that the amount of imaging probe gradually increased in the tumor tissue and mirrored by a decrease in the liver after the injection (Figure 5E). The ratio of tumor to normal tissue is more than 3 after 24 hours and lasted at least 120 hours after probe injection (Figure 5, panel D). Most interestingly, once the probe penetrated into the center (necrotic) areas of the tumor, it was retained there for as long as 120 hours (Figure 5B). The center area of the tumor was confirmed by histology as necrotic tumor tissue (arrow head in Figure 5C). Cell debris was also seen in the boundary between tumor and necrotic tissue (open arrow in panel C). Living tumor cells were also observed around blood vessels (solid arrow in panel C).

Discussion

Ovarian cancer remains the leading cause of death from a cancer of gynecologic origin and the fourth most common cause of cancer death in women worldwide [24]. The primary reason for this high mortality is that most ovarian cancer patients are diagnosed at a late stage [3]. Most patients with advanced disease will relapse within 5 years after initial treatment. Early detection and localization of small or subclinical (occult) tumors [25], specifically identifying subcentimeter peritoneal implants, is a significant adverse factor in the treatment of this disease [26]. Computerized tomography (CT) is a commonly used imaging technique in the clinic, but it frequently fails to identify tumors less than 1 cm in diameter owing to the low contrast of metastatic deposits relative to the normal peritoneal and serosal surface [27-29]. Furthermore, CT images cannot reflect alterations in tumor functional status that occur after cytotoxic therapy. In contrast, functional imaging techniques, such as radioimmunoscintigraphy and PET/CT, can accurately localize the tumor and provide additional biological information about this cancer. The functional imaging techniques require tumor specific binding ligands such as peptides and antibodies.

Antigens on the cell surface are easily accessible for binding ligands including antibodies for tumor targeted imaging and therapy. The binding of Mab CC188 to living (cultured) cells indicates that the epitope recognized by the antibody is localized on the cell membranes because living cells only allow surface molecules to be detected in the immunofluorescent staining. The intact cell membranes in living cells prevent IgG (150KD) from entering the cells passively. The internalization of Mab CC188 is also a remarkable feature which favors intracellular delivery of anticancer drugs. Most interestingly, Mab CC188 binds to ovarian CD133 + (cancer stem) cells which are believed to be initiating cells of primary, local recurrent and metastatic tumors, and responsible for resistance to conventional chemo- and radiotherapies [7,20]. Thereby, developing imaging reagents aimed at CSCs could facilitate small tumor detection and improve the survival of cancer patients [30]. CD133 is relatively well documented as a biomarker for ovarian CSCs [31-36]. Significant numbers of CD133+ cells co-express CD44/CD117 molecules which are suggested to be CSC biomarkers [33]. Studies have shown that a single CD133 positive cell can develop two population of cells, CD133+ and CD133- cell population. In contrast, a single CD133- cell can only develop CD133-cell population [32]. For these reasons, ovarian cancer CD133+ cells should be

targeted by imaging reagents for early tumor detection. Despite the key roles played by CSCs in tumor initiation, development and resistance to chemo- and radiotherapies, antibody based tumor targeting therapeutic reagents that are presently used either do not directly target tumor cells or inefficiently target CSCs [37]. For example, Bevacizumab, an antibody approved by the FDA, targeting vascular endothelial growth factor receptor (VEGFR) inhibits tumor growth mainly through the mechanism of anti-angiogenesis [37]. Epithelial growth factor receptor (EGFR) targeted by Trastuzumab and Cetuximab approved by FDA is not strongly expressed in CSCs [38].

Tumor and normal tissue array analysis demonstrate that about 75% of human ovarian cancer tissue samples are stained with Mab CC188, while peripheral blood mononuclear cells (PBMCs), hematopoietic stem (CD34+) cells and most normal tissues are negative with Mab CC188 staining [23]. These results imply that the Mab CC188 is an ideal candidate for developing biological imaging and therapeutic reagents for ovarian cancer early discovery and treatment.

Diffusion, clearance and cellular internalization of imaging probes determine their biodistribution and kinetic changes *in vivo*. In this study, we have observed that the probes penetrate throughout the tumor within 24 hours post injection, particularly diffusing into the tumor core and/or necrotic areas. Moreover, the probe is retained in the tumor tissue for at least 120 hours. We found that once the imaging probes reach the core and/or tissue necrotic areas, they accumulate and are retained there for a longer period of time than when they are bound to peripheral tumor tissues and excretory organs such as the liver and kidney. Mab CC188 based imaging and therapeutic reagents may be capable of detecting subclinical tumors *in vivo* and efficiently delivering anti-cancer drugs to the tumor cells localized in the boundary regions of necrotic tissue and tumor tissue. These regions supposedly contain abundant quiescent/CSC cells [18,39,40]. Antibody based imaging and therapeutic reagents have advantages and disadvantages in tumor targeted imaging and therapy. The conjugates of antibody with imaging agents and anti-cancer drugs generally have higher binding affinity and specificity. They are also retained in the tumor for a much longer time compared to small peptide based imaging and therapeutic reagents. The disadvantage is that longer time is required for clearance from normal cells and tissues including blood and excretory organs. There are also some concerns about diffusion of antibody based imaging and therapeutic reagents into deep tumor tissues where there is a higher interstitial fluid pressure and heterogeneous blood supply [41,42]. However, our results demonstrate that Mab CC188-NIR conjugates penetrated into the necrotic tumor tissues within 24 hours. Furthermore, to shorten the clearance time and reduce the binding of antibody based imaging and therapeutic reagents to normal tissue, other investigators have developed several tumor pre-targeting systems and IgG fragments based imaging and therapeutic reagents such as Fab, F(ab')₂, scFv, diabodies and minibodies [43,44]. In a future study, it would be interesting to inoculate ovarian CSCs into nude mice to develop a xenograft which will contain more CSCs [32] for the feasibility study of the imaging and therapeutic reagents *in vivo*. Furthermore, antibody conjugated with NIR imaging probes may be useful for identifying subclinical implants on peritoneal regions before and during surgery. In addition, the antibody could be labeled with radionuclide to detect small tumors using nuclear imaging. Many ovarian cancer patients including stage I patients have subclinical (unsuspected) metastasis [45,46]. Identifying subclinical tumors will help the physician to properly manage the disease because the subclinical tumor influences patient survival [47-49].

Acknowledgments

This work was supported in part by the GCF (Gynecologic Cancer Foundation/Gail MacNeil KOH Early Detection of Ovarian Cancer research grant) and the US National Institutes of Health grants R01 EB008111 and R01 EB008458.

References

1. <http://www.atihhealthnet.com/pages/ovariancancer.html>.
2. Besancon R, Valsesia-Wittmann S, Puisieux A, de Fromental CC, Maguer-Satta V. Cancer stem cells: the emerging challenge of drug targeting. *Curr Med Chem*. 2009; 16:394–416. [PubMed: 19199913]
3. Nossov V, Amneus M, Su F, Lang J, Janco JM, Reddy ST, Farias-Eisner R. The early detection of ovarian cancer: from traditional methods to proteomics. Can we really do better than serum CA-125? *Am J Obstet Gynecol*. 2008; 199:215–23. [PubMed: 18468571]
4. Heintz AP, Odicino F, Maisonneuve P, Quinn MA, Benedet JL, Creasman WT, Ngan HY, Pecorelli S, Beller U. Carcinoma of the ovary. FIGO 26th Annual Report on the Results of Treatment in Gynecological Cancer. *Int J Gynaecol Obstet*. 2006; 95(Suppl 1):S161–92. [PubMed: 17161157]
5. Clarke-Pearson DL. Clinical practice. Screening for ovarian cancer. *N Engl J Med*. 2009; 361:170–7. [PubMed: 19587342]
6. Bast RC Jr, Brewer M, Zou C, Hernandez MA, Daley M, Ozols R, Lu K, Lu Z, Badgwell D, Mills GB, Skates S, Zhang Z, et al. Prevention and early detection of ovarian cancer: mission impossible? *Recent Results Cancer Res*. 2007; 174:91–100. [PubMed: 17302189]
7. Azad NS, Annunziata CM, Steinberg SM, Minasian L, Premkumar A, Chow C, Kotz HL, Kohn EC. Lack of reliability of CA125 response criteria with anti-VEGF molecularly targeted therapy. *Cancer*. 2008; 112:1726–32. [PubMed: 18300236]
8. Hensley ML. A step forward for two-step screening for ovarian cancer. *J Clin Oncol*. 28:2128–30. [PubMed: 20368556]
9. Yurkovetsky Z, Skates S, Lomakin A, Nolen B, Pulsipher T, Modugno F, Marks J, Godwin A, Gorelik E, Jacobs I, Menon U, Lu K, et al. Development of a multimarker assay for early detection of ovarian cancer. *J Clin Oncol*. 28:2159–66. [PubMed: 20368574]
10. Karam AK, Karlan BY. Ovarian cancer. The duplicity of CA125 measurement. *Nat Rev Clin Oncol*. 7:335–9. [PubMed: 20368726]
11. Anastasi E, Marchei GG, Viggiani V, Gennarini G, Frati L, Reale MG. HE4. A new potential early biomarker for the recurrence of ovarian cancer. *Tumour Biol*. 2010; 31:113–9. [PubMed: 20358424]
12. He RH, Yao WM, Wu LY, Mao YY. Highly elevated serum CA-125 levels in patients with non-malignant gynecological diseases. *Arch Gynecol Obstet*. 2011; 283S:S107–10.
13. Turk HM, Pekdemir H, Buyukberber S, Sevinc A, Camci C, Kocabas R, Tarakcioglu M, Buyukberber NM. Serum CA 125 levels in patients with chronic heart failure and accompanying pleural fluid. *Tumour Biol*. 2003; 24:172–175. [PubMed: 14654710]
14. Sjovall K, Nilsson B, Einhorn N. The significance of serum CA 125 elevation in malignant and nonmalignant diseases. *Gynecol Oncol*. 2002; 85:175–8. [PubMed: 11925140]
15. Kim YM, Whang DH, Park J, Kim SH, Lee SW, Park HA, Ha M, Choi KH. Evaluation of the accuracy of serum human epididymis protein 4 in combination with CA125 for detecting ovarian cancer: a prospective case-control study in a Korean population. *Clin Chem Lab Med*. 2011; 49:527–34. [PubMed: 21320028]
16. Van Gorp T, Cadron I, Despierre E, Daemen A, Leunen K, Amant F, Timmerman D, De Moor B, Vergote I. HE4 and CA125 as a diagnostic test in ovarian cancer: prospective validation of the Risk of Ovarian Malignancy Algorithm. *Br J Cancer*. 2011; 104:863–70. [PubMed: 21304524]
17. Shahi MH, Schiapparelli P, Afzal M, Sinha S, Rey JA, Castresana JS. Expression and epigenetic modulation of sonic hedgehog-GLI1 pathway genes in neuroblastoma cell lines and tumors. *Tumour Biol*. 2011; 32:113–27. [PubMed: 20830616]

18. Grainger SJ, Serna JV, Sunny S, Zhou Y, Deng CX, El-Sayed ME. Pulsed ultrasound enhances nanoparticle penetration into breast cancer spheroids. *Mol Pharm.* 2010; 7:2006–19. [PubMed: 20957996]
19. Bhosale P, Peungjesada S, Wei W, Levenback CF, Schmeler K, Rohren E, Macapinlac HA, Iyer RB. Clinical utility of positron emission tomography/computed tomography in the evaluation of suspected recurrent ovarian cancer in the setting of normal CA-125 levels. *Int J Gynecol Cancer.* 2010; 20:936–44. [PubMed: 20683399]
20. Ricci-Vitiani L, Lombardi DG, Pilozzi E, Biffoni M, Todaro M, Peschle C, De Maria R. Identification and expansion of human colon-cancer-initiating cells. *Nature.* 2007; 445:111–5. [PubMed: 17122771]
21. Ricci-Vitiani L, Pagliuca A, Palio E, Zeuner A, De Maria R. Colon cancer stem cells. *Gut.* 2008; 57:538–48. [PubMed: 18334662]
22. <http://www.atihhealthnet.com/pages/ovariancancer.html> :
23. Xu M, Yuan Y, Xia Y, Achilefu S. Monoclonal antibody CC188 binds a carbohydrate epitope expressed on the surface of both colorectal cancer stem cells and their differentiated progeny. *Clin Cancer Res.* 2008; 14:7461–9. [PubMed: 19010863]
24. <http://www.cdt-babes.ro/medical-articles/ovarian-cancer-diagnostic-tests.php>:
25. Gadducci A, Cosio S, Zola P, Landoni F, Maggino T, Sartori E. Surveillance procedures for patients treated for epithelial ovarian cancer: a review of the literature. *Int J Gynecol Cancer.* 2007; 17:21–31. [PubMed: 17291227]
26. Chi DS, Eisenhauer EL, Lang J, Huh J, Haddad L, Abu-Rustum NR, Sonoda Y, Levine DA, Hensley M, Barakat RR. What is the optimal goal of primary cytoreductive surgery for bulky stage IIIc epithelial ovarian carcinoma (EOC)? *Gynecol Oncol.* 2006; 103:559–64. [PubMed: 16714056]
27. Kyriazi S, Kaye SB, deSouza NM. Imaging ovarian cancer and peritoneal metastases--current and emerging techniques. *Nat Rev Clin Oncol.* 7:381–93. [PubMed: 20386556]
28. Jacquet P, Jelinek JS, Steves MA, Sugarbaker PH. Evaluation of computed tomography in patients with peritoneal carcinomatosis. *Cancer.* 1993; 72:1631–6. [PubMed: 8348494]
29. de Bree E, Koops W, Kroger R, van Ruth S, Witkamp AJ, Zoetmulder FA. Peritoneal carcinomatosis from colorectal or appendiceal origin: correlation of preoperative CT with intraoperative findings and evaluation of interobserver agreement. *J Surg Oncol.* 2004; 86:64–73. [PubMed: 15112247]
30. Surwit EA, Childers JM, Krag DN, Katterhagen JG, Gallion HH, Waggoner S, Mann WJ Jr. Clinical assessment of ¹¹¹In-CYT-103 immunoscintigraphy in ovarian cancer. *Gynecol Oncol.* 1993; 48:285–92. [PubMed: 8462896]
31. Ferrandina G, Bonanno G, Pierelli L, Perillo A, Procoli A, Mariotti A, Corallo M, Martinelli E, Rutella S, Paglia A, Zannoni G, Mancuso S, Scambia G. Expression of CD133-1 and CD133-2 in ovarian cancer. *Int J Gynecol Cancer.* 2008; 18:506–14. [PubMed: 17868344]
32. Baba T, Convery PA, Matsumura N, Whitaker RS, Kondoh E, Perry T, Huang Z, Bentley RC, Mori S, Fujii S, Marks JR, Berchuck A, et al. Epigenetic regulation of CD133 and tumorigenicity of CD133+ ovarian cancer cells. *Oncogene.* 2009; 28:209–18. [PubMed: 18836486]
33. Curley MD, Therrien VA, Cummings CL, Sergent PA, Koulouris CR, Friel AM, Roberts DJ, Seiden MV, Scadden DT, Rueda BR, Foster R. CD133 expression defines a tumor initiating cell population in primary human ovarian cancer. *Stem Cells.* 2009; 27:2875–83. [PubMed: 19816957]
34. Ferrandina G, Martinelli E, Petrillo M, Prisco MG, Zannoni G, Sioletic S, Scambia G. CD133 antigen expression in ovarian cancer. *BMC Cancer.* 2009; 9:221. [PubMed: 19583859]
35. Kusumbe AP, Mali AM, Bapat SA. CD133-expressing stem cells associated with ovarian metastases establish an endothelial hierarchy and contribute to tumor vasculature. *Stem Cells.* 2009; 27:498–508. [PubMed: 19253934]
36. Bapat SA, Mali AM, Koppikar CB, Kurrey NK. Stem and progenitor-like cells contribute to the aggressive behavior of human epithelial ovarian cancer. *Cancer Res.* 2005; 65:3025–9. [PubMed: 15833827]
37. Culy C. Bevacizumab. *Antiangiogenic cancer therapy. Drugs Today (Barc).* 2005; 41:23–36. [PubMed: 15753967]

38. Yasuda H, Tanaka K, Saigusa S, Toiyama Y, Koike Y, Okugawa Y, Yokoe T, Kawamoto A, Inoue Y, Miki C, Kusunoki M. Elevated CD133, but not VEGF or EGFR, as a predictive marker of distant recurrence after preoperative chemoradiotherapy in rectal cancer. *Oncol Rep.* 2009; 22:709–17. [PubMed: 19724847]
39. Heddleston JM, Li Z, Lathia JD, Bao S, Hjelmeland AB, Rich JN. Hypoxia inducible factors in cancer stem cells. *Br J Cancer.* 102:789–95. [PubMed: 20104230]
40. Das B, Tsuchida R, Malkin D, Koren G, Baruchel S, Yeger H. Hypoxia enhances tumor stemness by increasing the invasive and tumorigenic side population fraction. *Stem Cells.* 2008; 26:1818–30. [PubMed: 18467664]
41. Jain RK, Baxter LT. Mechanisms of heterogeneous distribution of monoclonal antibodies and other macromolecules in tumors: significance of elevated interstitial pressure. *Cancer Res.* 1988; 48:7022–32. [PubMed: 3191477]
42. Jain RK. Physiological barriers to delivery of monoclonal antibodies and other macromolecules in tumors. *Cancer Res.* 1990; 50:814s–9s. [PubMed: 2404582]
43. DeNardo SJ. Radioimmunodetection and therapy of breast cancer. *Semin Nucl Med.* 2005; 35:143–51. [PubMed: 15765377]
44. Bell A, Wang ZJ, Arbabi-Ghahroudi M, Chang TA, Durocher Y, Trojahn U, Baardsnes J, Jaramillo ML, Li S, Baral TN, O'Connor-McCourt M, Mackenzie R, et al. Differential tumor-targeting abilities of three single-domain antibody formats. *Cancer Lett.* 2009; 289:81–90. [PubMed: 19716651]
45. Piver MS, Barlow JJ, Lele SB. Incidence of subclinical metastasis in stage I and II ovarian carcinoma. *Obstet Gynecol.* 1978; 52:100–4. [PubMed: 683618]
46. Herzog TJ, Coleman RL, Markman M, Cella D, Thigpen JT. The role of maintenance therapy and novel taxanes in ovarian cancer. *Gynecol Oncol.* 2006; 102:218–25. [PubMed: 16460787]
47. Gershenson DM, Copeland LJ, Wharton JT, Atkinson EN, Sneige N, Edwards CL, Rutledge FN. Prognosis of surgically determined complete responders in advanced ovarian cancer. *Cancer.* 1985; 55:1129–35. [PubMed: 3155643]
48. Podratz KC, Malkasian GD Jr, Wieand HS, Cha SS, Lee RA, Stanhope CR, Williams TJ. Recurrent disease after negative second-look laparotomy in stages III and IV ovarian carcinoma. *Gynecol Oncol.* 1988; 29:274–82. [PubMed: 3345949]
49. Rubin SC, Hoskins WJ, Saigo PE, Chapman D, Hakes TB, Markman M, Reichman B, Almadrones L, Lewis JL Jr. Prognostic factors for recurrence following negative second-look laparotomy in ovarian cancer patients treated with platinum-based chemotherapy. *Gynecol Oncol.* 1991; 42:137–41. [PubMed: 1894172]

Abbreviations

CSCs	Cancer stem cells
CT	computerized tomography
EGFR	Epithelial growth factor receptor
FCS	Fetal bovine serum
Mab	Monoclonal antibody
NIR	Near infrared
PBMCs	peripheral blood mononuclear cells
PET	positron emission tomography
VEGFR	Vascular endothelial growth factor receptor

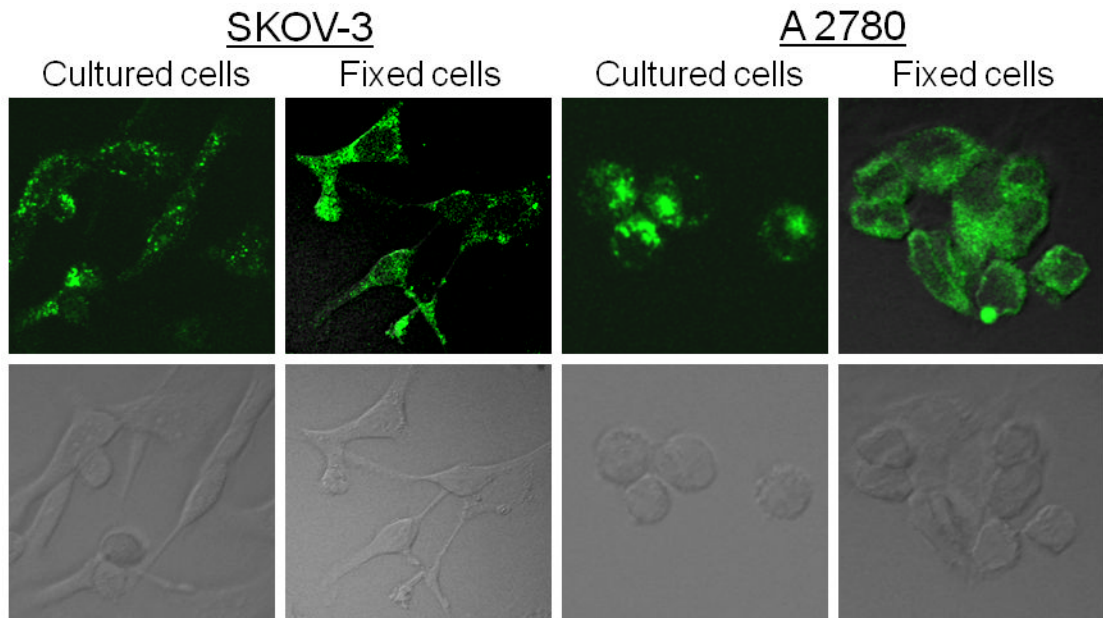


Figure 1. Fluorescence confocal microscopy of ovarian cancer cells stained with Mab CC188. The antibody stains both living (cultured) and 4% paraformaldehyde fixed SKOV-3 and A2780 human ovarian cancer cells. Upper panels are dark field. Lower panels are bright field controls.

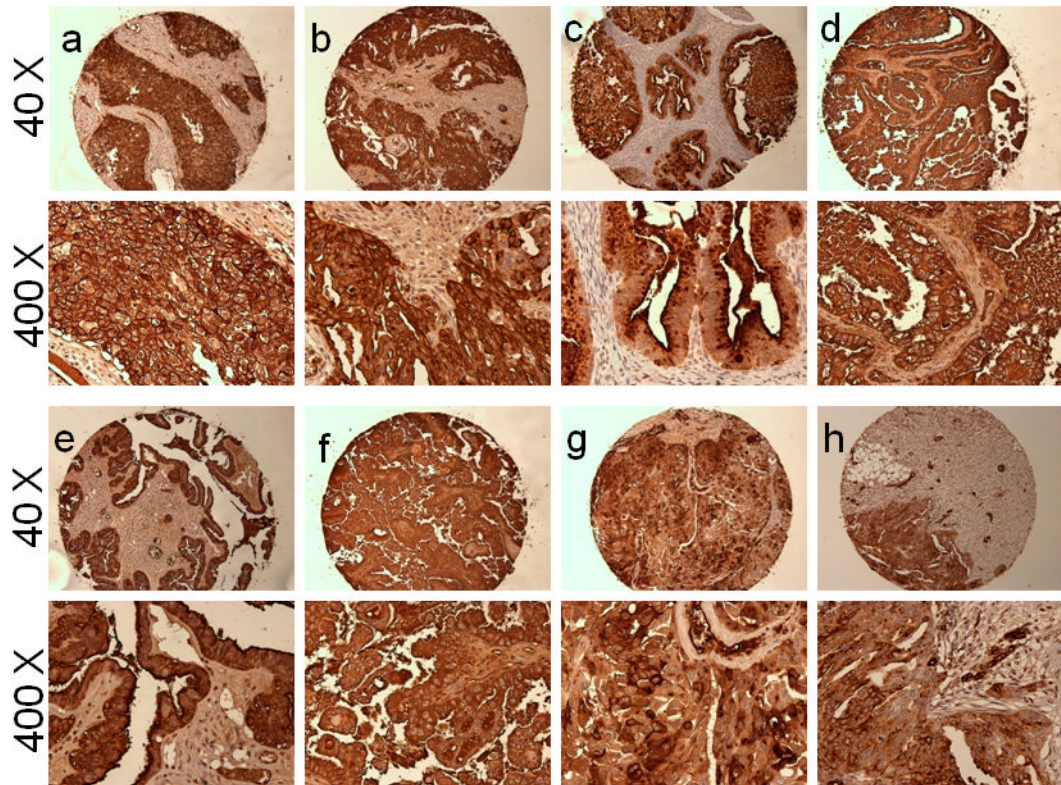


Figure 2. Immunohistochemical staining of Mab CC188 in human ovarian cancer tissues: Mab CC188 specifically, intensively and homogeneously stains different histological types of ovarian tumor cells, such as serous adenocarcinoma (Panels a and b); endometrioid adenocarcinoma (c); Serous papillary adenocarcinoma (d and e) and mucinous adenocarcinomas (g and h).

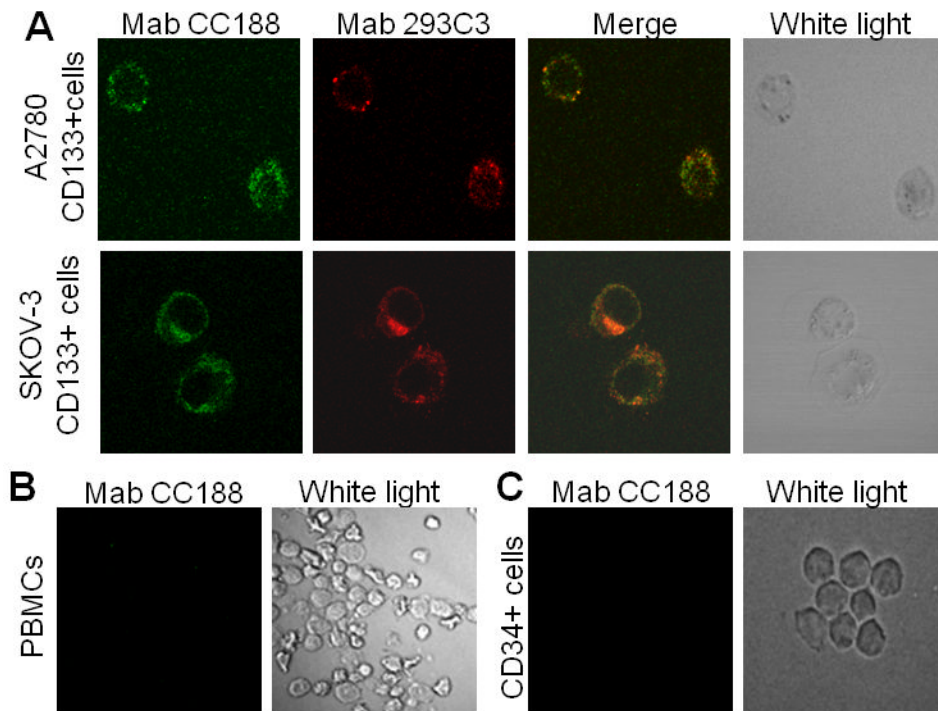


Figure 3.
 A: Dual immunofluorescence staining of ovarian cancer stem (CD133 +) cells using Mab 293C3 conjugated with Phycoerythrin (PE, red) to CD133 secondary binding site and Mab CC188 labeled with Alexa Fluor 488 (green). Dual color staining images are analyzed with a sequential program from Olympus FV 1000 microscope software. Figure 3. B and C: Immunofluorescence staining of PBMCs and hemato-poietic stem (CD34+) cells respectively with Mab CC188 labeled Alexa Fluor 488 (green).

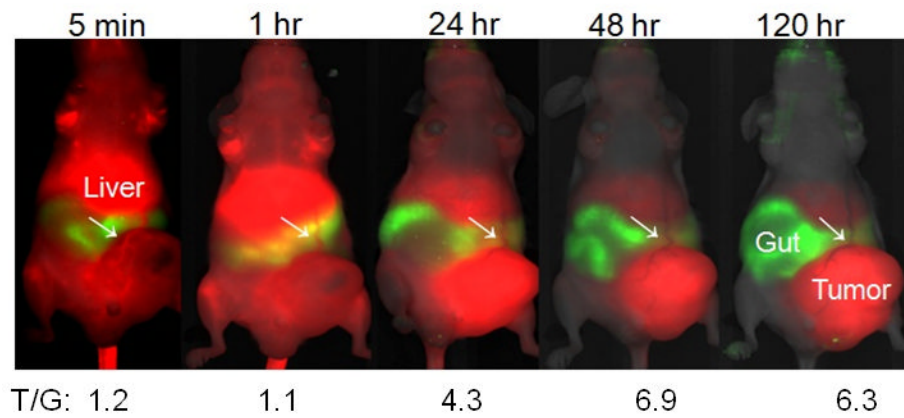


Figure 4.

Optical imaging of a mouse with human ovarian xenograft tumor. Shown are kinetic changes of Mab CC188- NIR dye IRDye 800CW conjugate in blood circulation. White arrows indicate blood vessels that supply nutrient and oxygen to the tumor. Red color indicates 800 nm channel (Mab-NIR dye probe), and green indicates 700 nm channel of gut fluorescence for contrast. The majority of the imaging probes is eliminated from circulation 24 hr post injection and completely removed from blood 48 hr after injection. T/G (Tumor / Gut) ratios are shown on the bottom of the images.

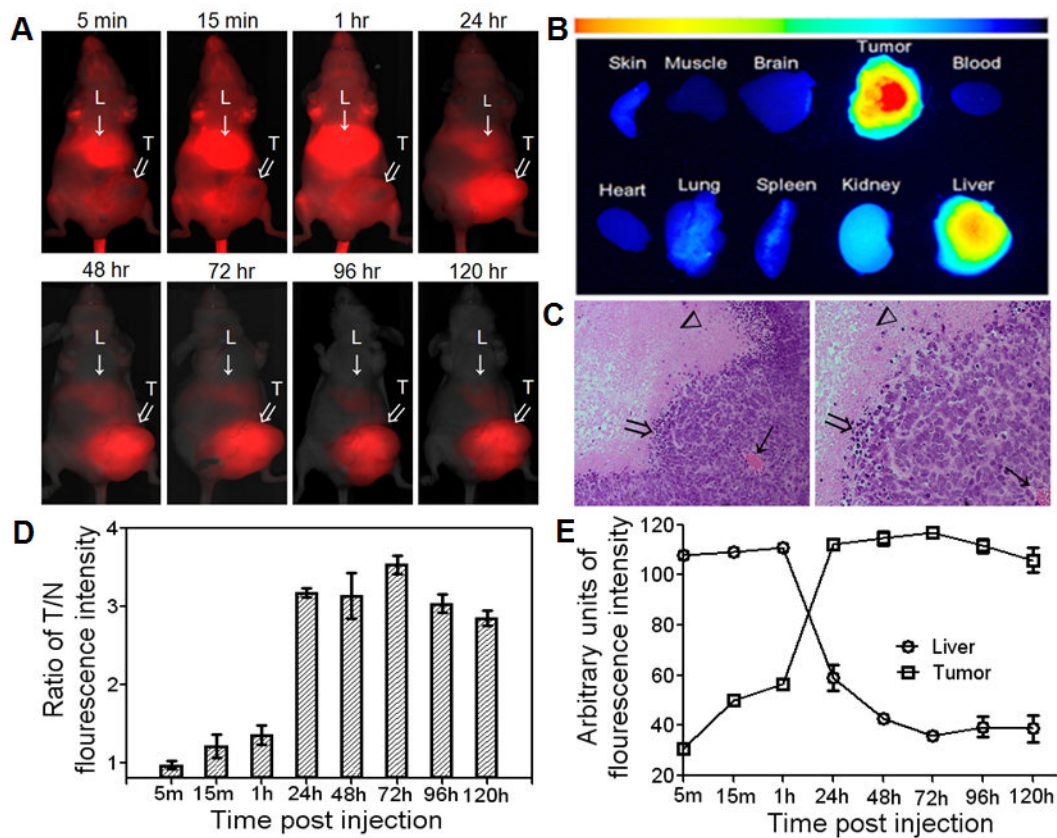


Figure 5. Optical images of human ovarian xenograft tumor in mouse; A: Optical images were generated using Pearl Imager (LI-COR Biosciences) after injection of Mab CC188 conjugated with NIR dye IRDye 800CW. Images were taken at different time points after tail vein injection of Mab CC188-NIR probes. “L” represents liver indicated by solid arrows. “T” represents tumor indicated by open white arrows. Panel B: Ex-vivo analysis of the probe biodistribution in the various mouse tissues and organs at 120 hours post injection. Panel C: H&E stained histological sections of the xenograft tumor, necrotic tissues are pink in color (arrow head), blood vessel indicated by solid arrow, inflammatory cells and cell debris indicated by open arrows in the boundary of tumor and necrotic tissues. Panel D: Fluorescence intensity ratios of tumor versus normal tissues which include skin, connective tissue and muscles in a region away from tumor and liver post injection of the antibody-NIR dye conjugates. Min: represents minutes and H: represents hours. Panel E: Kinetic changes of Mab CC188-NIR dye conjugates in excretory organ (liver) and xenograft tumor after the injection.